Atomic and electronic structures of the ordered $2\sqrt{3}\times2\sqrt{3}$ and molten 1×1 phase on the Si(111):Sn surface

P. E. J. Eriksson,[1] J. R. Osiecki,[1] Kazuyuki Sakamoto,[2] and R. I. G. Uhrberg[1]
[1]*Department of Physics, Chemistry and Biology, Linköping University, S-581 83 Linköping, Sweden*
[2]*Graduate School of Advanced Integration Science, Chiba University, Chiba 263-8522, Japan*
(Received 22 February 2010; published 7 June 2010)

The Si(111) surface with an average coverage of slightly more than one monolayer of Sn, exhibits a $2\sqrt{3}\times2\sqrt{3}$ reconstruction below 463 K. In the literature, atomic structure models with 13 or 14 Sn atoms in the unit cell have been proposed based on scanning tunneling microscopy (STM) results, even though only four Sn atoms could be resolved in the unit cell. This paper deals with two issues regarding this surface. First, high-resolution angle-resolved photoelectron spectroscopy (ARPES) and STM are used to test theoretically derived results from an atomic structure model comprised of 14 Sn atoms, ten in an underlayer and four in a top layer [C. Törnevik, M. Hammar, N. G. Nilsson, and S. A. Flodström, Phys. Rev. B **44**, 13144 (1991)]. Low-temperature ARPES reveals six occupied surface states. The calculated surface band structure only reproduces some of these surface states. However, simulated STM images show that certain properties of the four atoms that are visible in STM are reproduced by the model. The electronic structure of the Sn atoms in the underlayer of the model does not correspond to any features seen in the ARPES results. STM images are presented which indicate the presence of a different underlayer consisting of eight Sn atoms, which is not compatible with the model. These results indicate that a revised model is called for. The second issue is the reversible transition from a $2\sqrt{3}\times2\sqrt{3}$ phase below 463 K to a 1×1 phase corresponding to a molten Sn layer, above that temperature. It is found that the surface band structure just below the transition temperature is quite similar to that at 100 K. The surface band structure undergoes a dramatic change at the transition. A strong surface state, showing a 1×1 periodicity, can be detected above the transition temperature. This state resembles parts of two surface states which, already before the transition temperature is reached, have begun a transformation and lost much of their $2\sqrt{3}\times2\sqrt{3}$ periodicities. Calculated surface band structures obtained from 1×1 models with one monolayer of Sn are compared with ARPES and STM results. It is found that the strong surface state present above the transition temperature shows a dispersion similar to that of a calculated surface band originating from the Sn-Si interface with the Sn atoms in T_1 sites.

DOI: 10.1103/PhysRevB.81.235410 PACS number(s): 73.20.At, 68.08.De, 79.60.−i, 68.37.Ef

I. INTRODUCTION

Sn-induced reconstructions on Si(111) are relatively well studied in surface science. It is, however, mainly the $\frac{1}{3}$ monolayer (ML) $\sqrt{3}\times\sqrt{3}$ phase, henceforth called $\sqrt{3}$, that has been investigated. The higher coverage $2\sqrt{3}\times2\sqrt{3}$ phase, $2\sqrt{3}$ for short, has not received that much attention and the surface structure is not yet fully established. The $2\sqrt{3}$ phase is difficult to produce without the coexistence of the $\sqrt{3}$ phase. According to Ichikawa,[1] the Si(111):Sn surface exhibits a $2\sqrt{3}$ reflection high-energy electron diffraction pattern at temperatures below 463 K with a Sn coverage (θ_{Sn}) of $0.3<\theta_{Sn}<1.1$ ML. But, with an average θ_{Sn} less than ~1.05 ML, the $2\sqrt{3}$ and $\sqrt{3}$ phases were reported to coexist. The $\sqrt{3}$ structure was found to be more stable than the $2\sqrt{3}$ phase and survived to a temperature of 1133 K, at which the diffraction pattern transformed into that of a 1×1 periodicity. At a coverage slightly higher than 1.1 ML, three reconstructions with larger unit cells were observed at room temperature (RT): $(\sqrt{133}\times4\sqrt{3})$, $(3\sqrt{7}\times3\sqrt{7})R(30^\circ\pm10.9^\circ)$, and $(2\sqrt{91}\times2\sqrt{91})R(30^\circ\pm3.0^\circ)$. The pure $2\sqrt{3}$ phase was only observed below 463 K with the average coverage in a narrow interval, approximately $1.05<\theta_{Sn}<1.1$ ML.

Based on scanning tunneling microscopy (STM) studies, the first model of the $2\sqrt{3}$ surface was proposed by Törnevik *et al.*[2] The unit cell contains two Sn layers with ten atoms in an underlayer and four in a top layer. However, only the top layer, with two pairs of atoms, could be resolved experimentally. Subsequent STM studies[3–6] have also failed to resolve the structure of the underlayer. The electronic structure of the $2\sqrt{3}$ surface has been investigated with scanning tunneling spectroscopy (STS),[4,6] angle-resolved photoelectron spectroscopy (ARPES),[6,7] and *k*-resolved inverse photoelectron spectroscopy (KRIPES) (Ref. 7) resulting in the identification of several filled and empty states near the Fermi level (E_F). However, no detailed study of the surface state dispersions has been published so far.

A characteristic feature of the Si(111):Sn surface is the abrupt and reversible phase transition[1] at around 463 K. The structural change, which is manifested by the switch between a $2\sqrt{3}$ and a 1×1 pattern in low-energy electron diffraction (LEED), is interesting since it could be used as a model system for studying surface melting. The lack of long-range order in liquids usually makes momentum space based techniques difficult to use. However, by supporting the liquid on the periodic lattice of a solid crystal, reciprocal-lattice vectors are introduced enabling the liquid to be studied with, e.g., ARPES, as shown for the Cu(111):Pb surface in Ref. 8. The melting transition on the Si(111):Sn surface has been observed before in STM,[5] but the literature is lacking reports on the effect of the phase transition on the surface band structure.

This paper presents a comparison between calculated atomic as well as electronic structures obtained from a $2\sqrt{3}$ model based on Ref. 2 and experimental ARPES, STM, and STS data. Six surface states are identified in the ARPES data from the $2\sqrt{3}$ phase at 100 K. Furthermore, we managed to image the underlayer using STM. Based on the information from the STM images we arrive at a structure of the underlayer that is different from that of Ref. 2. However, the atomic structure of this underlayer remains somewhat uncertain since our calculations have been unable to identify a stable atomic configuration. The $2\sqrt{3} \leftrightarrow 1 \times 1$ transition is studied and the electronic structure of the surface slightly below and slightly above the transition temperature is presented. The surface band structure just below the phase transition is found to be similar to the one at 100 K. Above the transition temperature the photoemission spectra are completely dominated by one strong surface state. Combined ARPES and STM results obtained at various temperatures are used to gain information on the nature of the transition and also to help with the identification of the surface states.

II. EXPERIMENTAL DETAILS

All photoemission measurements were performed at the MAX-lab synchrotron radiation facility in Lund, Sweden. Linearly polarized light from the MAX-III storage ring was used for the ARPES measurements at beamline I4. For the low-temperature ARPES study a fixed Specs Phoibos 100 analyzer was used, resulting in energy and angular resolutions of about 50 meV and $\pm 0.1°$, respectively. ARPES data at elevated temperatures were obtained using a VG ARUPS 10 analyzer mounted on a goniometer and the energy and angular resolutions were 50 meV and $\pm 2°$, respectively. The Si(111) sample (n doped, Sb, 3 Ω cm) was cut from a single crystal wafer. Sample cleaning was done by direct resistive heating, reaching a temperature of 1530 K, at which the sample was held for a few seconds before it was allowed to cool down slowly. As observed by LEED and by Si $2p$ core-level spectroscopy, this procedure resulted in a nice 7×7 reconstructed surface. Sn was deposited from an evaporation source at a rate of approximately $\frac{1}{3}$ ML/min. A sharp $2\sqrt{3}$ LEED pattern was observed at RT after annealing at 900 K for 2 min. Sn was removed from the surface by annealing the sample at 1220 K for 30 s between preparations. During Sn evaporation and measurements the pressure in the vacuum system was below 2×10^{-10} torr. For the measurements at elevated temperatures, a custom built heating device was used. The device alternated, with a kilohertz frequency, between (1) passing the heating current through the sample while blocking the signal from the electron analyzer to the data taking computer and (2) grounding the sample while acquiring data. To prevent accumulation of heat in the sample holder it was cooled with liquid nitrogen. The Fermi energy of a Ta foil in electrical contact with the sample was used as reference in the ARPES data.

The quality of the $2\sqrt{3}$ surface prepared for the photoemission study was determined by inspection of the LEED pattern. To ensure that measurements were performed exclusively on the $2\sqrt{3}$ phase, the sample was prepared in such a way that neither the $\sqrt{3}$ phase was observed at temperatures above 463 K, nor were any reconstructions with larger unit cells[1] visible in LEED at RT. For the STM and STS study the sample was prepared in a similar way, but additional preparations with lower Sn coverage were also performed to allow for simultaneous studies of the $2\sqrt{3}$ and $\sqrt{3}$ phases. In the STM and STS study, a vacuum system equipped with an Omicron VT-STM and a LEED was used. The STM was operated in a constant current mode using W tips prepared by electrochemical etching. The tips were additionally cleaned *in situ* by electron-beam heating.

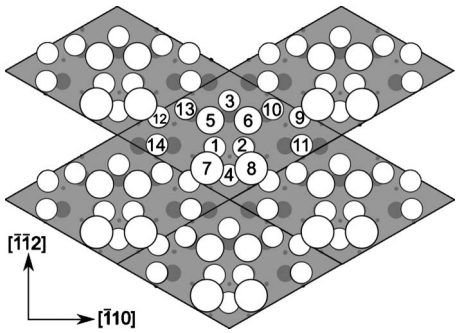

FIG. 1. Atomic configuration after relaxation of the $2\sqrt{3}$ model based on Ref. 2. Open circles, gray circles, and dots indicate the positions of Sn atoms, first layer Si atoms, and second layer Si atoms, respectively.

III. COMPUTATIONAL DETAILS

All theoretical results were obtained by density-functional theory calculations in the generalized gradient approximation[9] using the full-potential (linearized) augmented plane-wave+local orbitals method within the WIEN2K code.[10] The atomic slabs used for the structure relaxation of the $2\sqrt{3}$ models, which had an inversion center in the middle and Sn on both surfaces, were constructed of 12 Si layers. A vacuum of 15 Å separated the slabs in the [111] direction. Usually five **k** points in the irreducible Brillouin zone and an energy cutoff of 72 eV were used. To avoid artificial splitting of the surface bands, the surface band-structure calculations were performed on a H-terminated slab with six Si layers using an energy cutoff of 99 eV. For the 1×1 model cases, a H-terminated slab with 12 Si layers was used.

IV. RESULTS AND DISCUSSION

A. Atomic and electronic structures

The use of high-resolution ARPES, in combination with calculated surface band structures, is a powerful method for investigating surface properties. A key factor is the atomic model used as input for the calculations. In this study a $2\sqrt{3}$ atomic structure based on the model in Ref. 2 was used in the calculations. Approximate atomic coordinates were extracted from Fig. 3(b) in Ref. 2. The structure was then subjected to a relaxation procedure. Residual forces were very small and the relaxed structure (see Fig. 1) remained very similar to that in Ref. 2. Relaxed coordinates are given in Table I. Con-

TABLE I. Coordinates of the Sn atoms 1–14 inside the diamond-shaped $2\sqrt{3}$ unit cell in Fig. 1. Lateral coordinates are given relative to the unrelaxed Si bulk truncated position near Sn atom 4. Interplanar coordinates are relative to the unrelaxed bulk truncated position of the atoms in the first Si layer.

	Position (Å)		
Atom	$[\bar{1}10]$	$[\bar{1}\bar{1}2]$	[111]
1	−1.49	3.13	2.74
2	1.49	3.13	2.74
3	0.00	8.01	2.69
4	0.00	0.24	2.84
5	−1.97	5.98	3.11
6	1.97	5.98	3.11
7	−2.29	0.95	4.55
8	2.29	0.95	4.55
9	7.35	6.29	2.75
10	4.53	7.15	2.70
11	7.50	3.38	2.21
12	−7.35	6.29	2.75
13	−4.53	7.15	2.70
14	−7.50	3.38	2.21
First layer Si			0.13[a] ±0.1

[a]Average value.

trary to earlier relaxations done on models based on Ref. 2 (see Refs. 5 and 11), we found that Sn atoms 7 and 8 protrude quite a lot from the surface. To verify that this was not a local minimum these two atoms were moved 1 Å closer to the surface and allowed to relax again. They were then found to return to their original positions. A different $2\sqrt{3}$ model was proposed in Ref. 5. By applying the relaxation procedure, this model was found to be modified in such a way that the atomic positions would not comply with the experimental STM images. Thus, only the model based on Ref. 2 was chosen for further investigations.

High-resolution ARPES data were acquired from a $2\sqrt{3}$ surface at 100 K using a photon energy of 27 eV. The data were processed using a Savitzky-Golay[12] method differentiating the data twice along the energy axis in order to produce a map, where the color represents the curvature of the original data. This procedure gives a dark color where there are sharp features in the data. Figure 2 shows a color map of the ARPES features along $\bar{\Gamma}$-$\bar{K}$-$\bar{M}$ of the 1×1 surface Brillouin zone (SBZ). As shown in the inset this is equivalent to a $\bar{\Gamma}$-$\bar{M}$ direction in the $2\sqrt{3}$ SBZ. The calculated valence-band maximum (VBM) is placed 0.19 eV below E_F. This value was deduced from a comparison of the energy position at $\bar{\Gamma}$ of the direct bulk transition, labeled B in Figs. 2 and 3, with data from a clean Si(111) 7×7 surface. The value $E_F-E_{VBM}=0.65$ eV for the clean surface[13] was used as reference.

Six surface bands S_1-S_6 either completely or partially in the gap of the bulk band projection were identified in the ARPES data (see Fig. 2). All of them show a periodicity of

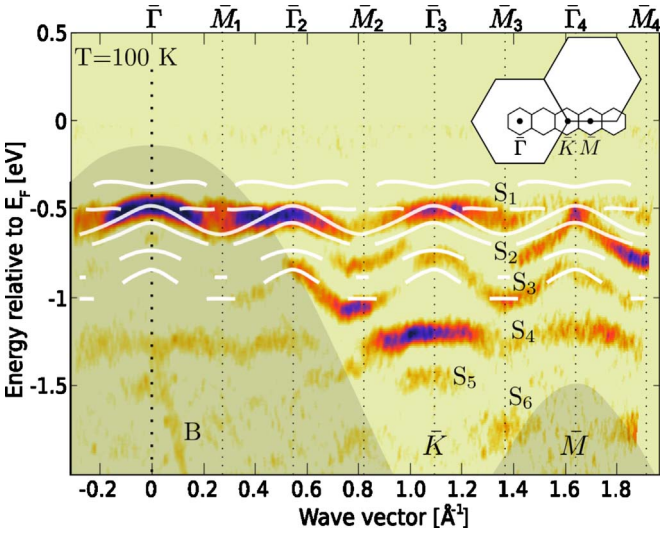

FIG. 2. (Color online) Band structure of the $2\sqrt{3}$ Si(111):Sn surface. Intensity in the color map indicates features in ARPES data ($h\nu=27$ eV) obtained at 100 K. Six surface states and one bulk feature are labeled S_1-S_6 and B, respectively. Calculated bands which show surface character are indicated by white curves. The shaded regions indicate the projection of the bulk bands. Vertical dotted lines indicate symmetry points in the $2\sqrt{3}$ SBZs.

0.55 Å^{-1}, which corresponds to the length of the $2\sqrt{3}$ reciprocal-lattice vector, $\bar{\Gamma}$-$\bar{M}$-$\bar{\Gamma}$. The S_1 state is visible in the whole $\mathbf{k}_\parallel$ range in Fig. 2. S_2-S_4 are mainly visible in the bulk band-gap region. S_5 only appears at $\bar{\Gamma}_3$, and S_6 is visible outside the projected bulk bands but only near $\bar{M}_3$ and $\bar{M}_4$. S_1-S_4 show a downward dispersion going from the center toward the edges of the $2\sqrt{3}$ SBZs. It is not possible to determine any dispersion of S_5 and S_6 since they are only visible in very limited $\mathbf{k}_\parallel$ intervals. The energies of the surface state dispersions at the symmetry points are summarized in Table II. In Fig. 3 a subset of the ARPES data, used for producing the dispersion plot in Fig. 2, shows the relative intensities of the surface states.

To facilitate a comparison with the experimental ARPES results, the surface band structure of the model in Fig. 1 was calculated. Several filled energy bands were found to exhibit surface character in parts of the $\mathbf{k}_\parallel$ interval shown in Fig. 2. Only the parts with surface character are included (see the white curves). Hence, most bands in Fig. 2 appear discontinuous. It should be mentioned that the filled bands show much weaker surface character compared to the empty bands (not included in the figure). Most prominent in the empty bands are the contributions from atoms 5 and 6 to the empty band closest to E_F. This will be discussed more in connection to the STM results later in this section. The calculated bands have been shifted, so that S_1 and the filled surface band closest to E_F, which shows a downward dispersion around $\bar{\Gamma}$ in the calculations, match in energy. No surface state with an upward dispersion, like the uppermost calculated surface band, is found in the ARPES data. The calculated bands are in general distributed over many Sn atoms. One exception is the continuous band overlapping S_1. It originates mainly from Sn atoms 7 and 8. There are several calculated bands

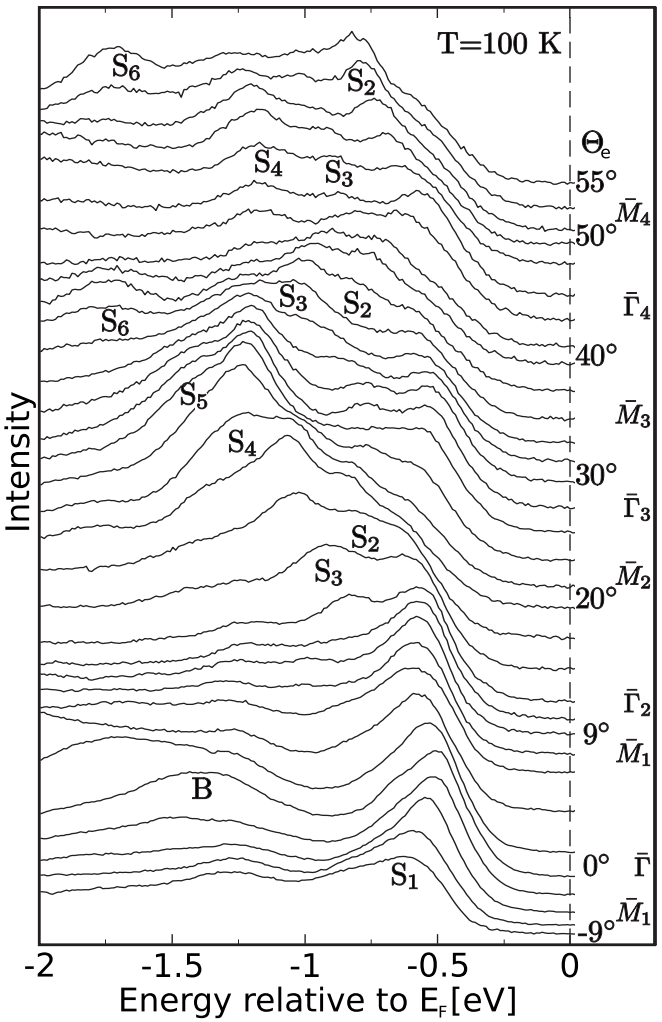

FIG. 3. Subset of the ARPES spectra ($h\nu$=27 eV, obtained at 100 K) used for creating the color map in Fig. 2. Six surface states S_1–S_6 and a bulk feature B are labeled. The emission angles Θ_e and the high-symmetry points, $\bar{\Gamma}$ and $\bar{M}$, of the $2\sqrt{3}$ SBZs have been labeled.

which show a downward dispersion around $\bar{\Gamma}$ and could explain S_2 and S_3. On the other hand, surface states S_4, S_5, and S_6 have no counterparts in the calculations. With all arguments considered, the match between the calculated surface bands and the ARPES data is poor. Since several ARPES states, among them the very strong S_4, were not described by the calculations we conclude that the model needs to be revised.

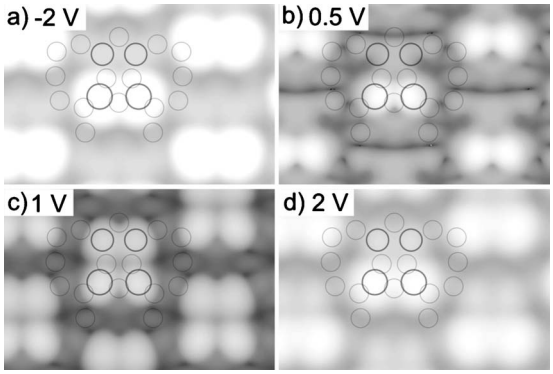

FIG. 4. Simulated constant current STM images at different biases from the model in Fig. 1. (a) Filled state image and (b)–(d) empty state images. The atomic configuration is shown with circles.

Some properties of the model were, however, found to be consistent with experimental STM results. They are mainly related to the empty states of the four top layer atoms. Constant current STM images were acquired from a sample prepared both with lower average Sn coverage than what was used for the ARPES study and with full coverage. The $2\sqrt{3}$ images were similar to what has been reported in previous publications.[2–6] Using the lower coverage surface enabled the study of areas with both the $\sqrt{3}$ and $2\sqrt{3}$ structures, simultaneously. It should be noted that the orientation of the $2\sqrt{3}$ cell with respect to the Si lattice was found to be the same as in Ref. 4, but 180° different from that in Ref. 2. In the atomic model based on Ref. 2 used in the present work the orientation is as observed in STM and reported in Ref. 4. Simulated STM images from the model in Fig. 1 are shown in Fig. 4. They do seem to reproduce features in the experimental data in several ways. The diffused appearance of the filled states are reproduced as a consequence of the delocalized and weak surface character of the filled bands. Filled state images are dominated by atoms 7 and 8 in STM, as well as in the calculated results as shown in Fig. 4(a). In the empty state images [see Figs. 4(b)–4(d)], the two pairs are easily recognized which reflects the much stronger, and more localized, nature of the empty states. These images show a larger variation with bias voltage compared to the filled state images.

Spatially resolved STS measurements were performed to help identify the origins of the different states in the ARPES data and to test the calculated surface band structure. Spatial resolution was achieved by probing a grid with 40×40 points spanning 50×50 Å^2. Figure 5(a) shows an averaged

TABLE II. Energies relative to E_F for the surface state bands S_1–S_6 in Fig. 2. The values have been measured at the symmetry points where the respective state appears the strongest.

	Energy relative to E_F (eV)					
$\mathbf{k}_\parallel$ point in the $2\sqrt{3}$ SBZ	S_1	S_2	S_3	S_4	S_5	S_6
$\bar{\Gamma}$	−0.51	−0.61	−0.82	−1.18		−1.38
$\bar{M}$	−0.61	−0.82	−1.10	−1.30	−1.72	

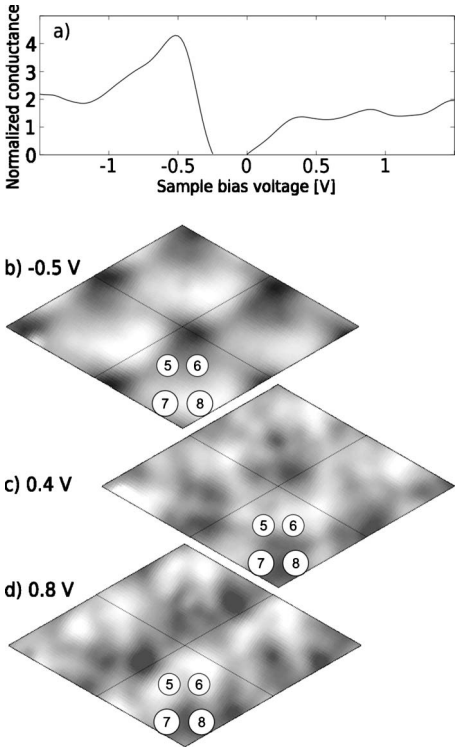

FIG. 5. STS data obtained at RT on the $2\sqrt{3}$ surface. (a) Averaged normalized conductance $\frac{dI}{dV}/\frac{I}{V}$ spectrum showing three features at −0.5, 0.4, and 0.8 V. (b)–(d) Spatially resolved STS maps of the normalized conductance at −0.5, 0.4, and 0.8 V, respectively.

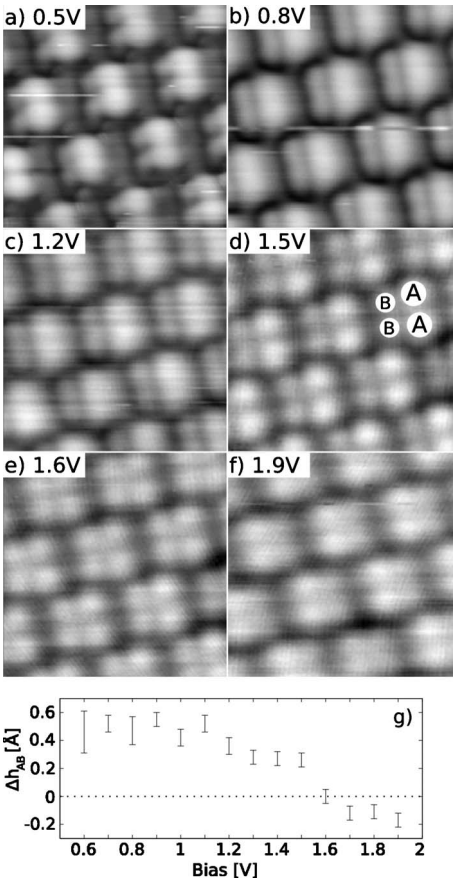

FIG. 6. (a)–(f) Empty state STM images obtained at 48 K, showing a 40×40 Å^2 area at various biases. The apparent height difference of the *AA* and *BB* pairs is displayed in (g). The error bars indicate the variation in apparent height difference at different positions in the images.

normalized conductance spectrum. Three features at −0.5, 0.4, and 0.8 V are observed. Their spatial distributions are shown in Figs. 5(b)–5(d). The density of states (DOS) increase at −0.5 V mainly originates from atoms 7 and 8 (Fig. 1), just like the calculated surface band at −0.5 eV in Fig. 2. The DOS increase at 0.4 V exhibits a nearly opposite behavior [see Fig. 5(c)]. There are bright areas near atoms 5 and 6. From the calculations this may be explained by the very strong contribution from atoms 5 and 6 to the empty bands close to E_F. At 0.8 V [Fig. 5(d)] the area near atoms 5 and 6 is again bright, but here it shows a tendency to stretch toward atoms 7 and 8. Also this can be expected from the model as calculated empty surface bands at higher energies are less localized at atoms 5 and 6 compared to the lower empty bands. The observations of the −0.5 and 0.4 V DOS features by STS are partially consistent with the STM and STS study in Ref. 6. There, a feature at −0.4 V was attributed to atoms 7 and 8, while a feature at 0.4 V was attributed collectively to atoms 5–8. The last feature in the DOS curve, at 0.8 V, is possibly the same as was seen in KRIPES in Ref. 7.

More STM support for the top layer structure in Fig. 1 was found in empty state images obtained at 48 K. Figures 6(a)–6(f) show such 40×40 Å^2 images. In Fig. 6(d), the two pairs in the unit cell, labeled *AA* and *BB*, are marked. They correspond to atoms 7 and 8, and 5 and 6 in Fig. 1, respectively. It was difficult to resolve the pairs in the upper and lower parts of the bias range, i.e., in Figs. 6(a) and 6(f), since the STM images show no clear minima between them. The apparent separation between the pairs was estimated to be around 4 Å, and in the middle of the bias range it measures 5.2 Å. The atoms in the *AA* pair appear as one broad feature for biases below 1.2 V. At higher biases the apparent *A*-*A* separation is around 5.3 Å. The apparent *B*-*B* separation is 4.6 Å, possibly slightly larger at biases close to 1.9 V. Also this pair appears as a single broad feature below 1.2 V, except at 0.5 V where a *B*-*B* separation of 4.3 Å can be resolved. The geometries of the *AA* and *BB* pairs are summarized in Table III. It is difficult to draw any conclusion on the z coordinate of the pairs due to the strong mixture of topographic and electronic contributions to the appearance of the pairs. Figure 6(g) shows the height difference between the *AA* and *BB* pairs at different biases. Usually the atoms in the *AA* pair appear larger, more separated, and higher than those in *BB*, but above 1.6 V the *BB* pair appears higher than *AA*. The bias at which the appearance changes was found to vary between 1.2 and 1.6 V depending on the position on the sample. A variation in apparent height could also be recognized in the simulated STM images in Fig. 4. At bias voltages around 1 V, the very strong empty state contribution from atoms 5 and 6 makes the *BB* pair appear almost as high as atoms 7 and 8 of the *AA* pair, despite a 1.44 Å height difference. In the calculations, the *AA* pair becomes dominant again at higher biases [Fig. 4(d)]. This behavior was not

TABLE III. In-plane geometrical parameters of the features observed in the STM images. *A-A*, *B-B*, and *A-B* refer to distances in Fig. 6. *a*–*h* refer to positional coordinates in Fig. 7(d).

Feature	Position (Å)		Feature	Distance (Å)
	x	*y*		
a	0.0	0.0	*A-A*	5.3 (>1.2 V)
b	0.3	4.9	*B-B*	4.6
c	5.7	0.2	*A-B*	5.2 (1.5 V)
d	6.0	5.1		≈4 (0.5 V, 1.9 V)
e	2.9	2.7		
f	2.4	7.7		
g	7.8	2.8		
h	7.7	7.9		

observed in the bias range used in the STM study.

B. STM of the Sn underlayer

Generally, it was found to be difficult to obtain images with sample bias voltages in the range $|V_{bias}|<0.5$ V. Often these lower biases resulted in irreversible changes to the tunneling conditions. However, at some parts of the sample it was possible to get atomic resolution using low biases. Figure 7(a) shows such an image recorded with 0.5 V bias. In the $2\sqrt{3}$ area the two pairs *AA* and *BB* can be resolved. The same area, but taken with 0.1 V bias, is shown in Fig. 7(b). In the image, a brighter pair similar to the *AA* pair is visible. The STM features are however slightly offset from where the *AA* pair would be. The *BB* pair is missing; instead new features have appeared in that area. The observation of the new features with a $2\sqrt{3}$ periodicity supports the idea that the reconstruction is composed of two layers: an underlayer and the top layer with the four atoms in the *AA* and *BB* pairs.

Another area was found which did not exhibit the usual $2\sqrt{3}$ pattern. It did not develop the structure with two pairs in empty state images and the features in the filled state images looked slightly different. When the bias was decreased this area changed gradually. Figure 7(c) shows an image at 0.1 V bias where features similar to those from the underlayer in Fig. 7(b) are clearly seen. The unit cell consists of seven well-resolved features, one of them so broad that we attribute it to two atoms. In Fig. 7(d) the eight atoms of the presumed underlayer are labeled *a*–*h*, where atoms *d* and *g* correspond to the broad feature. Their positions, relative to atom *a*, are given in Table III. Comparing with the usual $2\sqrt{3}$ surface in Refs. 2, 5, and 6 it seems like the surface in Fig. 7(c) has lower coverage. Here, an underlayer with eight atoms has been formed, but the top layer is missing. Using the $\sqrt{3}$ area in Figs. 7(a) and 7(b) it is possible to determine the relative positions of the top layer, the underlayer, and the $\frac{1}{3}$ ML T_4 sites occupied by Sn on the $\sqrt{3}$ area. Figure 7(e) shows a sketch of the underlayer and the top layer (open and solid gray circles, respectively) drawn on a grid which corresponds to the positions of Sn atoms (T_4 sites) in the $\sqrt{3}$ area.

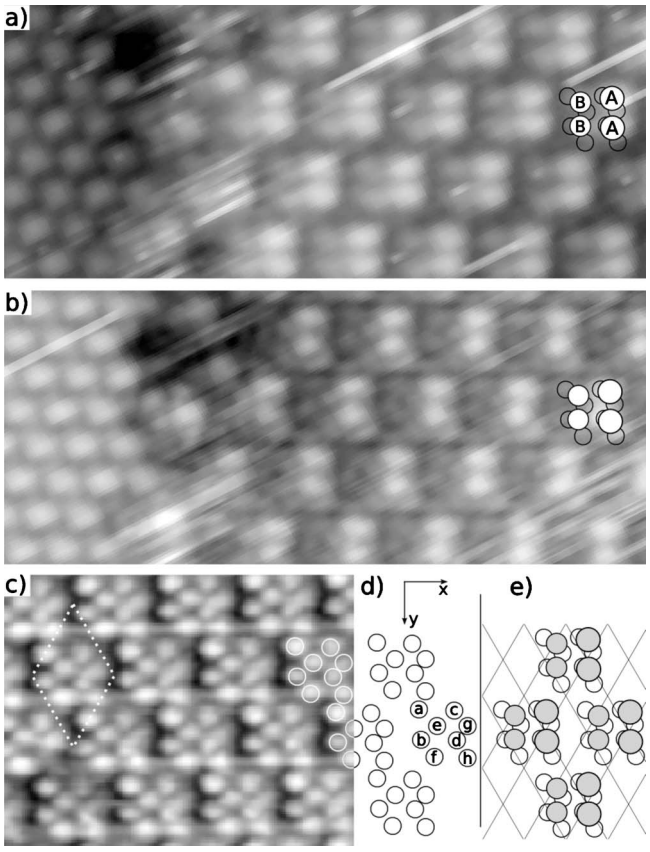

FIG. 7. RT STM images suggesting the presence of a double layer $2\sqrt{3}$ structure. (a) and (b) show the same area at 0.5 and 0.1 V sample biases, respectively. To the left is an adjacent $\sqrt{3}$ area. In (a) the *AA* and *BB* pairs in the top layer are visible. In (b) the *AA* pair and the underlayer are visible. (c) Image at 0.1 V bias of a different area where an eight-atom underlayer is clearly seen. (d) Atomic positions of the underlayer. (e) The underlayer and top layer (open and solid gray circles, respectively). The grid vertices correspond to the positions of the Sn atoms in the $\sqrt{3}$ area (T_4 sites).

The geometries of the two layers are shown to the right in Figs. 7(a) and 7(b). The top layer shows no symmetry with respect to the T_4 sites. The atomic configuration in Fig. 7(e) is inconsistent with the model in Fig. 1. These results call for a modified model. Force relaxations performed on models with only a base layer of eight Sn atoms in a $2\sqrt{3}$ unit cell have not resulted in any stable atomic configuration which laterally reproduces Fig. 7(d). A revised model of the $2\sqrt{3}$ unit cell with full coverage would consist of the modified underlayer with eight Sn atoms and four Sn atoms in a top layer, i.e., a coverage of 1.0 ML. This is consistent with previously reported estimates of the average coverage, e.g., 1.17 (Ref. 2) and 1.08 ML.[5]

C. $2\sqrt{3}\leftrightarrow 1\times 1$ phase transition

The $2\sqrt{3}$ surface is known[1] to undergo a reversible transition at 463 K. LEED patterns in Figs. 8(a) and 8(b) show the $2\sqrt{3}$ and the 1×1 periodicities of the surface below and above the transition temperature, respectively. Based on the difference in heating powers, compared to the power needed

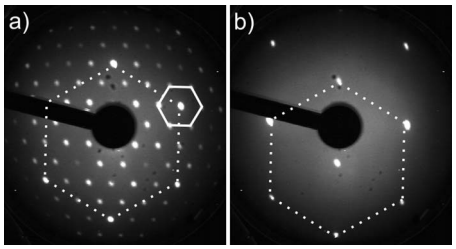

FIG. 8. Si(111):Sn LEED patterns obtained with a 95 eV electron-beam energy. The 1×1 and $2\sqrt{3}$ unit cells are shown by dotted and solid lines, respectively. (a) $2\sqrt{3}$ surface at a temperature slightly below 463 K. (b) 1×1 surface at a temperature slightly above 463 K. The LEED patterns appear shifted due the applied voltage associated with the resistive heating of the sample.

to reach the transition temperature, the actual sample temperatures were estimated to be a few tens of kelvins below and above the transition temperature, respectively. The surface phase transition was found to be very abrupt, reversible, and reproducible.

To investigate the effect of the phase transition on the electronic structure of the surface, ARPES was performed in the $\bar{\Gamma}$-$\bar{M}$ direction of the $2\sqrt{3}$ SBZ, i.e., the same direction as was investigated in the low-temperature measurements. As in the LEED study, ARPES spectra were recorded with the sample both slightly below and slightly above the transition temperature. Figure 9 shows ARPES spectra of the surface taken using a photon energy of 27 eV. Figure 9(a) shows spectra taken just below the transition temperature. These spectra are similar to those in Fig. 3, albeit less well resolved due to the higher temperature. Figure 9(b) shows spectra taken just above the transition temperature. Compared to the spectra in Fig. 9(a), most of the features are gone. It is not likely that the temperature difference between Figs. 9(a) and 9(b) alone is responsible for the change in the spectra since it is estimated to be quite moderate. The dispersions of the features in the spectra in Figs. 9(a) and 9(b) are shown by color maps in Figs. 10(a) and 10(b), respectively. Concurrent with the surface transition is a shift of the bulk band structure relative to E_F. It is observed by comparing the energy of the bulk feature labeled B at $\bar{\Gamma}$. In the $2\sqrt{3}$ data B is 1.46 eV below E_F, while in the 1×1 data it has shifted to 1.26 eV below E_F. By using the same method of calibrating with the bulk feature B, as was discussed in connection with Fig. 2, the calculated valence-band maxima were positioned 280 and 80 meV below E_F for the $2\sqrt{3}$ and 1×1 phases, respectively. Dotted curves labeled S_1–S_6 in Fig. 10(a) represent the surface state dispersions from the low-temperature ARPES data in Fig. 2. Thermal broadening makes it difficult to recognize all the individual surface bands S_1–S_6 in Fig. 10(a). It is however apparent that the electronic structure of the surface just below the transition temperature is similar to the one at 100 K, but it shows a significantly less pronounced $2\sqrt{3}$ periodicity.

In the surface band structure above the transition temperature [Fig. 10(b)], S_1, S_2, and S_6 are completely missing. S_5 was seen as a very weak shoulder on S_4 at 100 K and it is impossible to say whether it disappeared before or during the transition. A strong feature S_4' is very similar to S_4 around $\bar{K}$, except for a 0.15 eV shift toward E_F. This energy position overlaps with the energy of S_3 in Fig. 10(a) and it is uncertain whether the apparent dispersion of S_4' in the $\mathbf{k}_\parallel$ interval between 0.6 and 0.8 Å^{-1} in Fig. 10(b) is the result of overlap of S_4 with remnants of an S_3-like band or if S_4' is a completely new continuous surface state band.

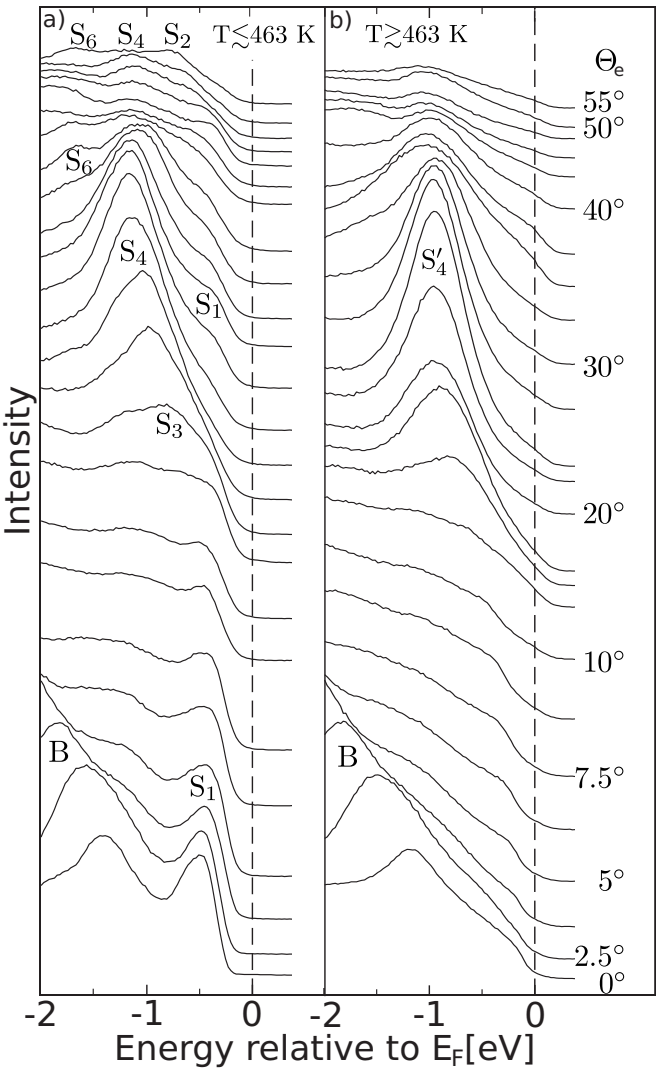

FIG. 9. ARPES spectra ($h\nu$=27 eV) obtained (a) slightly below and (b) slightly above the phase transition. Surface states identified from Fig. 2 are labeled S_1–S_4 and S_6; a bulk feature is labeled B.

An STM image showing the surface at the transition temperature can give a hint on the nature of the transition. In the left part of the filled state STM image in Fig. 11(a), the surface has undergone the melting transition and no structure can be resolved. The right part still shows the $2\sqrt{3}$ phase. A larger area which has not undergone the transition is shown in Fig. 11(b). The two pairs are recognized as two almost indistinguishable oblong features with an apparent height difference of less than 0.1 Å. The appearance of the BB pair in filled state images is drastically different from images obtained at RT, where only the AA pair could be seen. Thermal motion of the atoms in the top layer cannot be the sole cause of such a considerable change in the apparent height differ-

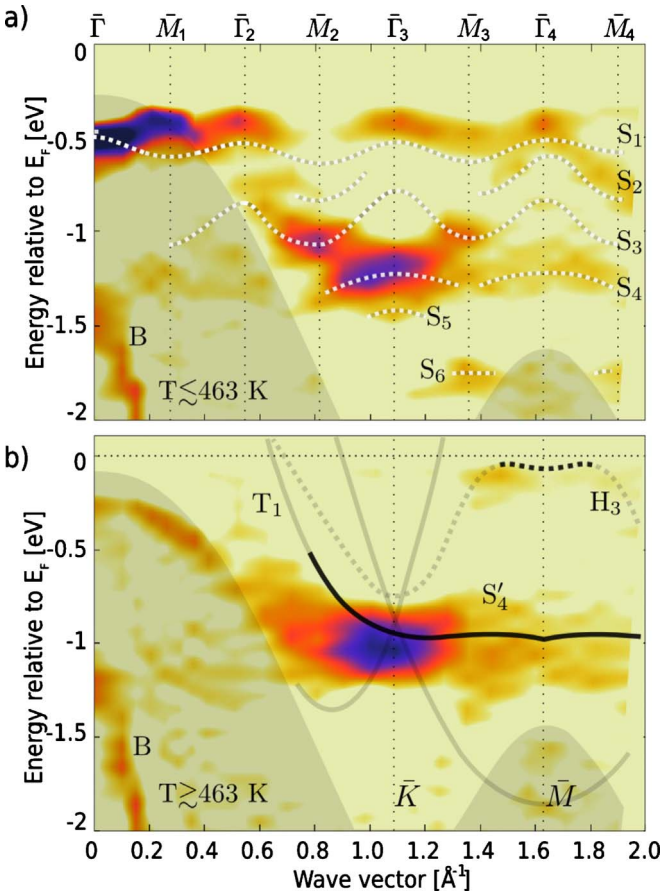

FIG. 10. (Color online) Color maps showing the dispersions of the features in the spectra in Fig. 9. (a) Slightly below the surface transition. Surface state dispersions from the $2\sqrt{3}$ surface at 100 K are drawn with dotted curves (cf. Fig. 2). (b) Slightly above the surface transition. Solid and dotted curves show calculated surface band dispersions from a 1×1 surface with 1 ML Sn at T_1 and H_3 sites, respectively. The parts of the bands that show p_z character are marked in black. The shaded region indicates the projection of the bulk bands. The calculated surface bands have been shifted down by about 0.1 eV, so that the energy position of the VBM in the band-structure calculations matches with the top of the projection of the bulk bands. Vertical dotted lines indicate symmetry points in the $2\sqrt{3}$ and 1×1 SBZs.

ence. Furthermore, no significant internal reorganization of the top layer atoms is expected as they still exhibit the pair structure. It is instead suggested that the underlayer has been changed, possibly due to thermal vibrations, thereby providing more similar sites for the two pairs to occupy. Conclusions on the origins of the surface states in the ARPES study can be drawn by considering the relation between the surface band structure and the abrupt structural change, from the reconstruction with the two pairs to what appears to be a molten phase with no structure in STM.

The concurrent disappearances of the pair structure and of the surface states S_1, S_2, and S_6, and possibly S_3 and S_5, suggest that these states are associated with the top layer atoms. The persistent ARPES feature S'_4 should be associated with the electronic structure of the Sn-Si interface.

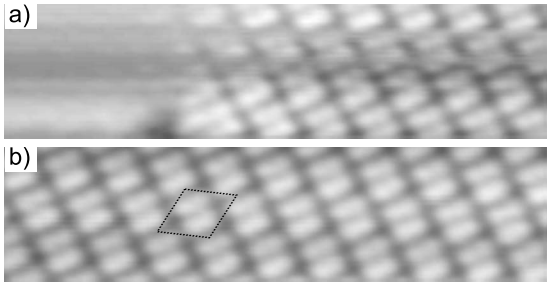

FIG. 11. Crops from a filled state STM image (−0.4 V sample bias) at the transition temperature. (a) In the left part the surface has undergone the transition and no longer shows any structure in STM. The right part still shows $2\sqrt{3}$ pattern. (b) Larger $2\sqrt{3}$ area showing the two pairs in the unit cell (dotted lines).

A state with a dispersion similar to that of S'_4 in Fig. 10(b) was found in model calculations made on Si(111) 1×1 unit cells with 1 ML of Sn. In the 1×1 unit cell, there are three high-symmetry sites for the Sn, namely, the T_1, H_3, and T_4 sites, corresponding to positions above first, fourth, and second layer Si atoms, respectively. Reedijk *et al.* showed in a diffraction study[14] that Sn on Ge(111), a system which exhibits a similar transition[1] as Sn on Si(111), can occupy all three sites. The T_1 sites were however preferable below as well as above the transition temperature. Above the transition, Sn atoms were reported to exhibit a mixture of solidlike and liquidlike behaviors as they diffuse on the surface but still showing a preference for the high-symmetry sites. In the case of the Si(111) surface with 1 ML of Sn, our total-energy comparisons reveal that T_1 sites are preferable over H_3 (+0.39 eV) and T_4 (+0.40 eV) sites. The best fit with ARPES data was found for the calculated surface band structures of the T_1 and H_3 cases. In Fig. 10(b), the black parts of the solid and dotted curves indicate where the surface bands show p_z character. The dispersion of S'_4 is quite well reproduced by the Sn-induced surface band in the T_1 case (solid black curve). Here, the Sn p_z orbital is part of the vertical Sn-Si bond. In addition, the black dotted curve which shows a calculated surface band with p_z character for the H_3 case could explain the very weak feature near E_F around $\bar{M}$. The solid and dotted gray curves represent calculated surface bands with p_x+p_y character for the T_1 and H_3 cases, respectively. These orbitals are mainly involved in lateral Sn-Sn bonds and has no counterpart in the ARPES data. This could partly be due to their very strong dispersion. Vibrations of the Sn atoms could also be expected to deform the Sn-Sn bonds which in turn would smear the electronic states. de Vries *et al.*[15] showed in a diffraction study on the similar Ge(111):Pb surface that in-plane vibrations are much stronger than vertical ones. This explains the coexistence of a smeared appearance of the surface, as shown in the left part of Fig. 11(a), and the presence of $\mathbf{k}_\parallel$-dependent surface states with strong p_z character.

The calculations on the 1×1 model systems are consistent with the ARPES and STM results in that they associate the persistent state with the Sn-Si interface. Furthermore, they identify the strong state above the transition temperature with the Sn-Si bond when Sn occupies T_1 sites.

V. SUMMARY

As a candidate to explain the atomic structure of the $2\sqrt{3}$ surface, the model proposed in Ref. 2 shows some qualities. Simulated STM images and atomic relaxation are fairly consistent with experimental STM images and STS data. The agreement with ARPES data is however questionable. With STM, an underlayer which could not be explained by the model was seen. The images do however confirm the idea that the structure is composed of two Sn layers. The underlayer appears to be constructed from eight Sn atoms. A revised model would then be composed of 12 Sn atoms per unit cell, i.e., a coverage of exactly 1.0 ML.

The $2\sqrt{3} \leftrightarrow 1\times1$ phase transition at 463 K was found to be accompanied by a dramatic change in the surface band structure. Just below the transition, ARPES shows surface bands that are quite similar to those obtained at 100 K. Above the transition temperature, the ARPES spectra are dominated by just one strong surface state S_4'. Model calculations show that the dispersion of the Sn-Si bond when Sn atoms occupy the T_1 sites in a 1×1 structure agrees with the dispersion of the S_4' state. A second weak surface state feature in the ARPES spectra was found to be consistent with a small number of Sn atoms in H_3 sites. The presence of $\mathbf{k}_\parallel$-dependent features also in the molten 1×1 phase indicates that it shows some solidlike behavior. Just above the transition temperature a significant fraction of the Sn atoms can be associated with T_1 sites.

ACKNOWLEDGMENTS

This work was financially supported by the Swedish Research Council (VR) and the Knut and Alice Wallenberg (KAW) Foundation. The calculations were performed on the Neolith cluster at the National Supercomputer Centre (NSC) in Linköping, Sweden.

[1] T. Ichikawa, Surf. Sci. **140**, 37 (1984).
[2] C. Törnevik, M. Hammar, N. G. Nilsson, and S. A. Flodström, Phys. Rev. B **44**, 13144 (1991).
[3] M. S. Worthington, J. L. Stevens, C. S. Chang, and I. S. T. Tsong, J. Vac. Sci. Technol. A **10**, 657 (1992).
[4] X. F. Lin, I. Chizhov, H. A. Mai, and R. F. Willis, Appl. Surf. Sci. **104-105**, 223 (1996).
[5] T. Ichikawa and K. Cho, Jpn. J. Appl. Phys. **42**, 5239 (2003).
[6] L. Ottaviano, G. Profeta, L. Petaccia, C. B. Nacci, and S. Santucci, Surf. Sci. **554**, 109 (2004).
[7] T. Kinoshita, H. Ohta, Y. Enta, Y. Yaegashi, S. Suzuki, and S. Kono, J. Phys. Soc. Jpn. **56**, 4015 (1987).
[8] F. Baumberger, W. Auwärter, T. Greber, and J. Osterwalder, Science **306**, 2221 (2004).
[9] J. P. Perdew, K. Burke, and M. Ernzerhof, Phys. Rev. Lett. **77**, 3865 (1996).
[10] P. Blaha, K. Schwarz, G. K. H. Madsen, D. Kvasnicka, and J. Luitz, *WIEN2K: An Augmented Plane Wave+Local Orbitals Program for Calculating Crystal Properties* (Karlheinz Schwarz, Tech. Universität Wien, Austria, 2001).
[11] C. L. Griffiths, H. T. Anyele, C. C. Matthai, A. A. Cafolla, and R. H. Williams, J. Vac. Sci. Technol. B **11**, 1559 (1993).
[12] A. Savitzky and M. J. E. Golay, Anal. Chem. **36**, 1627 (1964).
[13] R. Losio, K. N. Altmann, and F. J. Himpsel, Phys. Rev. B **61**, 10845 (2000).
[14] M. F. Reedijk, J. Arsic, F. K. de Theije, M. T. McBride, K. F. Peters, and E. Vlieg, Phys. Rev. B **64**, 033403 (2001).
[15] S. A. de Vries, P. Goedtkindt, P. Steadman, and E. Vlieg, Phys. Rev. B **59**, 13301 (1999).